AJNR

Utility of Photon-Counting Detector CT Myelography for the Detection of CSF-Venous Fistulas

A.A. Madhavan, L. Yu, W. Brinjikji, J.K. Cutsforth-Gregory, F.R. Schwartz, I.T. Mark, J.C. Benson and T.J. Amrhein

AJNR Am J Neuroradiol published online 18 May 2023
http://www.ajnr.org/content/early/2023/05/18/ajnr.A7887

Published May 18, 2023 as 10.3174/ajnr.A7887

Utility of Photon-Counting Detector CT Myelography for the Detection of CSF-Venous Fistulas

A.A. Madhavan, L. Yu, W. Brinjikji, J.K. Cutsforth-Gregory, F.R. Schwartz, I.T. Mark, J.C. Benson, and T.J. Amrhein

ABSTRACT

SUMMARY: CSF-venous fistulas are an increasingly recognized type of CSF leak that can be particularly challenging to detect, even with recently improved imaging techniques. Currently, most institutions use decubitus digital subtraction myelography or dynamic CT myelography to localize CSF-venous fistulas. Photon-counting detector CT is a relatively recent advancement that has many theoretical benefits, including excellent spatial resolution, high temporal resolution, and spectral imaging capabilities. We describe 6 cases of CSF-venous fistulas detected on decubitus photon-counting detector CT myelography. In 5 of these cases, the CSF-venous fistula was previously occult on decubitus digital subtraction myelography or decubitus dynamic CT myelography using an energy-integrating detector system. All 6 cases exemplify the potential benefits of photon-counting detector CT myelography in identifying CSF-venous fistulas. We suggest that further implementation of this imaging technique will likely be valuable to improve the detection of fistulas that might otherwise be missed with currently used techniques.

ABBREVIATIONS: CTM = CT myelography; CVF = CSF-venous fistula; DSM = digital subtraction myelography; EID = energy-integrating detector; LDDSM = lateral decubitus digital subtraction myelography; PCD = photon-counting detector; SIH = spontaneous intracranial hypotension; SR = standard resolution; T3D = low-energy threshold; UHR = ultra-high-resolution mode; VMI = virtual monoenergetic image

Spontaneous intracranial hypotension (SIH) is caused by a spinal CSF leak from a dural tear (type 1), leaking meningeal diverticulum (type 2), or a CSF-venous fistula (CVF, type 3).[1] Localization of the causative CSF leak requires imaging techniques with high spatial and temporal resolution, such as decubitus digital subtraction myelography (DSM) and dynamic CT myelography (CTM).[2,3] CVFs can be particularly challenging to detect because they may opacify with contrast only intermittently, and they sometimes require very dense intrathecal contrast for the draining vein to become visible. Procedural modifications such as imaging during inspiration and use of conebeam CT with DSM have recently been shown to increase the yield of detecting CVFs.[4-6] Despite optimal techniques, however, CVFs are sometimes missed.

Photon-counting detector (PCD) CT is a recent advancement that has multiple benefits over conventional energy-integrating detector (EID) CT.[7,8] EIDs convert incident x-rays into visible light, which subsequently encounters a photodiode that generates an electric signal proportional to the total energy deposited. As a result of this process, the energy information of each individual x-ray photon is lost. In contrast, PCDs convert the energy of each individual x-ray photon directly into an electric pulse and record the energy information on the basis of the pulse height, allowing more precise discrimination of individual photon energy. This photon-counting process permits a more optimal energy-weighting of individual photons and leads to multiple benefits over EIDs. First, electronic noise is substantially reduced by applying a low-energy threshold, leading to improved signal- and contrast-to-noise ratios. Second, photons can be binned into different energy ranges, and subsequent postprocessing can be performed to obtain virtual monoenergetic images (VMIs) without impairing scan speed or increasing the dose. The SNR of the VMIs is also typically better than can be achieved with modern dual-energy CT. Finally, because PCDs do not require physical septa between detector elements, detector pixel size can be made smaller compared with EIDs, yielding superior spatial resolution (up to 40 line pairs/cm). Due to these advantages, PCD CTM can theoretically detect CVFs that may not be apparent on DSM or EID CTM. One case of a CVF seen on PCD CTM has been reported, but its added value over DSM and EID CTM is yet to be demonstrated.[9]

Here, we report 6 cases of CVFs that were identified on PCD CT. The CVFs were occult on decubitus DSM or EID CTM in 5 cases.

Received March 15, 2023; accepted after revision April 26.

From the Division of Neuroradiology (A.A.M., L.Y., W.B., I.T.M., J.C.B.), Department of Radiology and Department of Neurology (J.K.C.-G.), Mayo Clinic, Rochester, Minnesota; and Division of Neuroradiology (F.R.S., T.J.A.), Department of Radiology, Duke University Medical Center, Durham, North Carolina.

Please address correspondence to Ajay Madhavan, MD, Division of Neuroradiology, Department of Radiology, Mayo Clinic, 200 First St SW, Rochester, MN 55905; e-mail: madhavan.ajay@mayo.edu

http://dx.doi.org/10.3174/ajnr.A7887

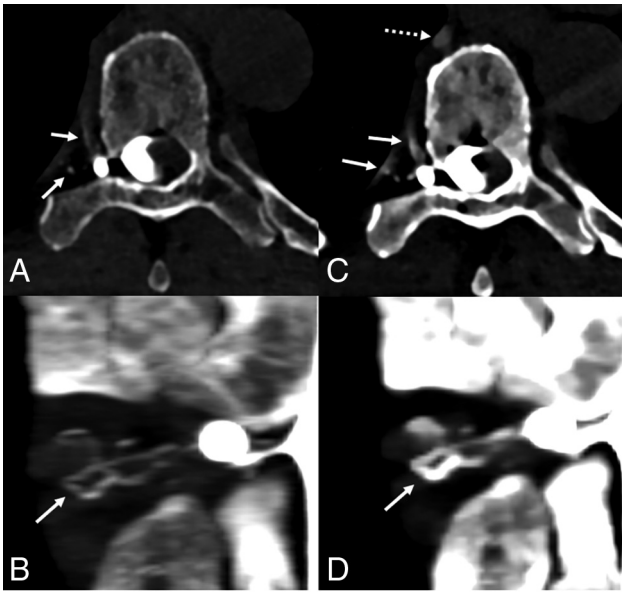

FIG 1. A 70-year-old man with 18 months of orthostatic headaches and brain MR imaging demonstrating diffuse pachymeningeal enhancement (not shown). Axial and coronal T3D reconstructions from a right lateral decubitus PCD CTM (*A* and *B*) at a section thickness of 0.2 mm demonstrate exquisite delineation of tiny veins draining a right T6 CVF (*A* and *B*, *arrows*). Axial and coronal 40-keV reconstructions at the identical time point and window/level settings, both at a section thickness of 0.4 mm (minimum allowable), demonstrate improved conspicuity of the iodine signal within the same veins (*C* and *D*, *solid arrows*) and within the more distal azygous vein (*C*, *dashed arrow*), though with slightly diminished anatomic characterization. PCD CT confers excellent spatial resolution and spectral information, which have a complementary role and can both be useful in imaging CVFs. The patient underwent transvenous Onyx embolization of the CVF.

MATERIALS AND METHODS

Patient Selection

This is a retrospective series including patients from 2 separate institutions specializing in the diagnosis and treatment of SIH. Medical records were searched for all consecutive patients who underwent PCD CTM for the indication of SIH from April 2022 to March 2023. All myelographic images, including EID CTMs, DSMs, and PCD CTMs were reviewed by 2 neuroradiologists blinded to the radiologic reports. Cases demonstrating a definitive CVF on PCD CTM were included in this case series. Clinical information and brain MR imaging findings from each included case were recorded. This study was deemed exempt by both institutional review boards.

Myelographic Examination Technique

The technique for lateral decubitus digital subtraction myelography (LDDSM) has been previously described and was used for the included patients.[10] For decubitus EID CTM, lumbar puncture was performed on the CT table, and 10–11 mL of iodinated contrast was injected immediately before performing a single scan of the entire spine. The needle was removed, and scanning was repeated with the patient in the contralateral decubitus position without injection of more contrast. The scanning protocol used a previously described technique.[3]

The PCD CTM technique varied slightly by participating institution. At the first institution, the patient was placed in the PCD CT scanner (NAEOTOM Alpha; Siemens) in the right lateral decubitus Trendelenburg position. A 20-ga spinal needle was advanced into the subarachnoid space at L3–L4 under CT guidance. Five milliliters of Omnipaque 300 (GE Healthcare) was injected intrathecally. Multiple low-dose monitoring scans at C7–T1 were performed every 5 seconds to dynamically monitor contrast flow. A series of 3–6 scans of the entire spine was initiated manually when intrathecal contrast reached C7–T1. All scans were performed at end inspiration with a 5-second interval between scans. The needle was removed, the patient was rotated to the left lateral decubitus position, and the process was repeated after placing a new spinal needle, injecting 5–6 mL of contrast, and performing 3–6 additional scans.

Among the 3–6 scans in each position, the first 2–4 scans were obtained with standard resolution (SR) mode (144 × 0.4 mm detector collimation), and the last 1–2 scans, with ultra-high-resolution (UHR) mode (120 × 0.2 mm detector collimation). All scans had a rotation time of 0.5 seconds, CAREkeV image quality level of 200. Automatic exposure control was on, with a manual kilovolt of 140. All scans were reconstructed separately at 40 keV, 55 keV, and at a low-energy threshold (referred to as T3D by the manufacturer and including photon energies from 20 keV to 140 keV), all with a Br40-3 kernel (quantum iterative reconstruction strength setting of 3). SR scans were reconstructed at 0.4 mm, and UHR scans were reconstructed at 0.2 mm. Pitch was 1.2 (SR) or 1.0 (UHR), and the mean time per scan was 5.0 seconds (SR) and 12.0 seconds (UHR).

At the second institution, lumbar puncture and contrast injection were performed under conventional fluoroscopy with a tilting table with the patient in the right lateral decubitus position, also at L3–L4 with an injection of 10 mL of Isovue-M 300 (Bracco). Patients were transferred to PCD CT while maintaining decubitus and Trendelenburg positioning, and a single scan in the UHR mode was obtained, in both cases approximately 10 minutes after contrast injection. Patients were rotated to the prone and left lateral decubitus positions, and 2 additional UHR scans were obtained in each position. Scans were reconstructed at 0.2 mm with T3D.

RESULTS

Patient Cohort

In total, 12 patients underwent PCD CTM during the study period (3 with prior negative findings on DSM, 8 with prior negative findings on EID CTM, and 1 with no prior myelographic studies). Of these, 6/12 had a definite CVF identified on PCD CTM by review of both neuroradiologists (figures/patients, 1–6), while the other 6 PCD CTMs had negative findings. In one of the cases with positive findings (patient 1), the PCD CTM was the first myelographic study performed. In another 3 patients (patients 2–4), LDDSM was performed initially and had negative findings. In the final 2 patients (patients 5 and 6), decubitus dynamic EID CTM was performed initially and had negative findings. Patients 1–4 were from the first institution, and patients 5 and 6 were from the second institution.

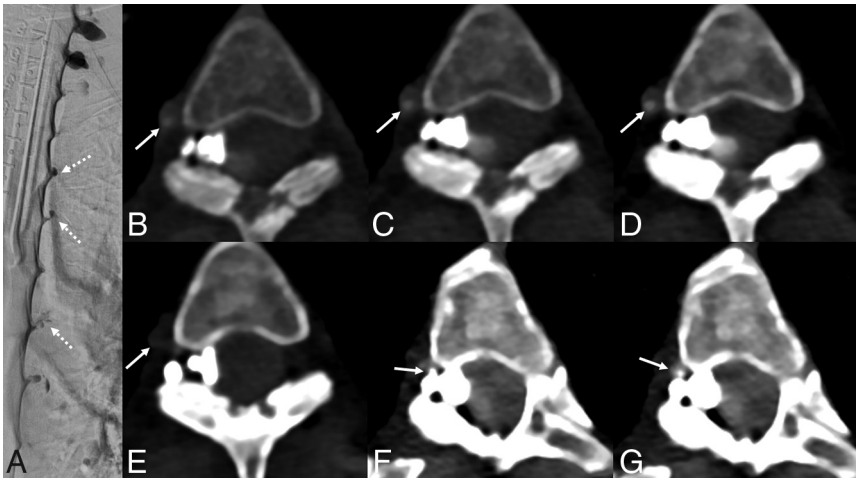

FIG 2. A 65-year-old woman with several years of orthostatic headaches and brain MR imaging demonstrating diffuse pachymeningeal enhancement and brain sag (not shown). Representative image from a right lateral decubitus DSM (*A*) shows multiple meningeal diverticula that remained stable during dynamic imaging (*A*, *dashed arrows*), with no evidence of a CVF. Axial images from a right lateral decubitus PCD CTM at the same time point (*B–D*) reconstructed at a T3D (*B*), 55 keV (*C*), and 40 keV (*D*) demonstrate a right T3 CVF (*B–D*, *arrows*), which is most apparent at 40 keV. The CVF is not apparent during imaging 30 seconds later, even at 40 keV (*E*, *arrow*). Additional images at adjacent slices, both from the earlier time point at 40 keV (*F* and *G*), show that this venous enhancement, though discontinuous, does, in fact, arise from a prominent meningeal diverticulum (*F* and *G*, *arrows*). In this case, the high degree of temporal resolution and spectral imaging conferred by PCD CT were necessary to confidently make the diagnosis. The patient underwent successful transvenous Onyx embolization of the right T3 CVF.

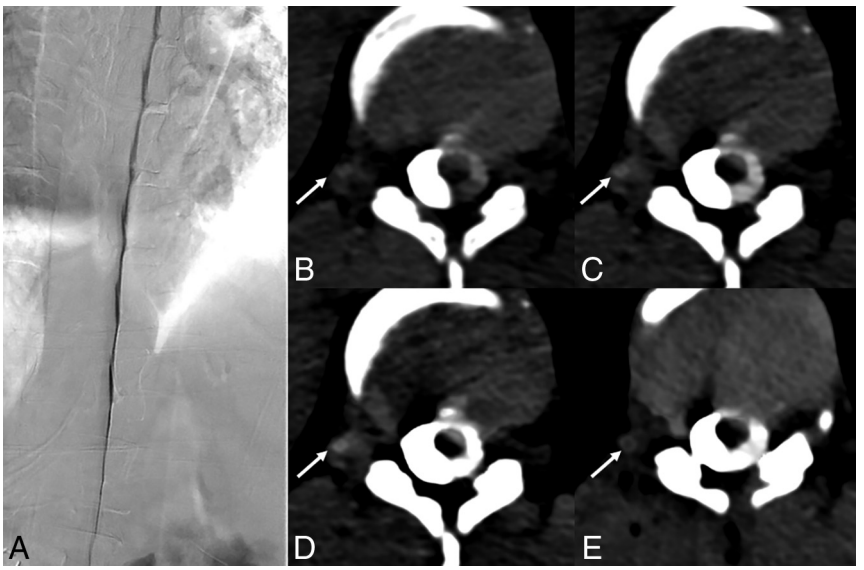

FIG 3. A 36-year-old woman with several years of orthostatic headaches, tinnitus, and MR imaging demonstrating brain sag without pachymeningeal enhancement (not shown). A representative image from a right lateral decubitus DSM (*A*) shows no evidence of a CVF. Axial images from a right lateral decubitus PCD CTM at the same time point (*B–D*) reconstructed at a T3D (*B*), 55 keV (*C*), and 40 keV (*D*) demonstrate a subtle right T11 CVF (*B–D*, *arrows*), most apparent at 40-keV. An axial 40-keV image obtained 20 seconds later (*E*) no longer shows this subtle venous opacification (*E*, *arrow*). The patient underwent Onyx embolization of this right T11 fistula.

Clinical and Conventional Imaging Findings

All 6 patients met International Classification of Headache Disorders (ICHD-3) criteria for SIH. Contrast-enhanced brain MR imaging showed brain sagging and/or pachymeningeal enhancement in patients 1, 2, 3, 5, and 6. Patient 4 had normal findings on brain MR imaging. All 6 patients had no evidence of extradural fluid on spine MR imaging (patients 1–4) or conventional CTM (patients 5 and 6).

Additional Advanced Myelography Findings

LDDSM for patients 2–4 and decubitus EID CTM for patients 5 and 6 were negative for CVF on review by both neuroradiologists. Although multiple meningeal diverticula were present, no levels had any findings suspicious for CVF or other leaks.

PCD CTM for all 6 patients was positive for a single definitive CVF on review by both neuroradiologists (Figs 1–6). In the cases from the first institution, the CVFs were most apparent at 40 keV using 0.4-mm reconstructions (Figs 1–4). In the cases from the second institution, the CVFs were most apparent using 0.2-mm T3D reconstructions (Figs 5 and 6). Mean dose-length product for patients 1–4 was 7223 mGy-cm, while the mean dose-length product for patients 5 and 6 was 1602 mGy-cm.

Treatment

Patients 1–4 underwent transvenous Onyx (Medtronic) embolization of their CVFs. Patients 5 and 6 underwent CT-guided epidural blood and fibrin glue patching at the level of the CVF. These are the preferred initial methods of treatment at each respective institution based on the availability of resources and institutional experience with each method of treatment. All patients have had symptomatic resolution to date, with the time since treatment ranging from 3 weeks to 6 months.

DISCUSSION

We have described 6 patients with SIH with CVFs identified using lateral decubitus PCD CTM. In 5 patients (patients 2–6), the CVF was occult using decubitus DSM or EID CTM. In all 6 cases, precise localization of the CVF on PCD CTM was instrumental in permitting targeted treatment.

Decubitus dynamic EID CTM and DSM are both excellent techniques for localization of CVFs.[3,10] Precise techniques for both modalities vary considerably across different institutions. Some of these variations include differences in timing between contrast injection and imaging, duration of imaging/frame rate (for DSM), number of scans obtained (for CTM),

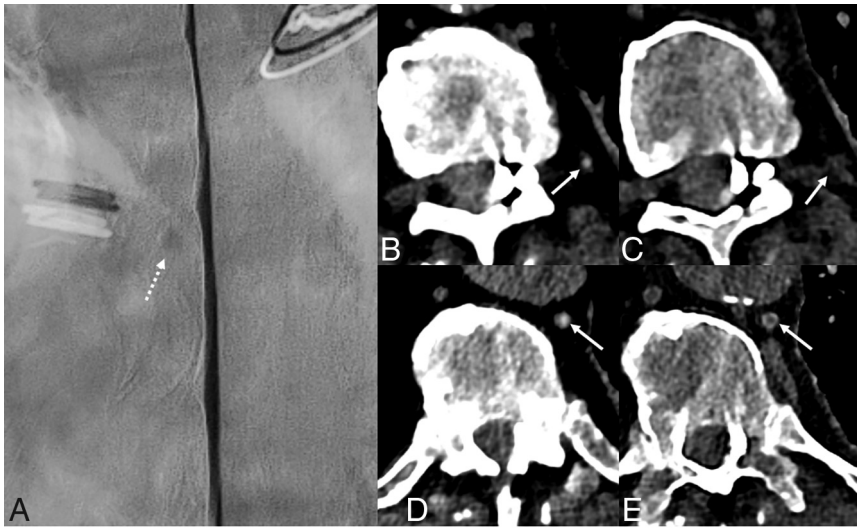

FIG 4. An 80-year-old man with several years of orthostatic headaches but normal brain MR imaging findings (not shown). Representative image from a left lateral decubitus DSM centered at T10 (*A*) shows a small meningeal diverticulum (*A*, *dashed arrow*) but no evidence of a CVF. Axial 40-keV images at 2 adjacent slices from a left lateral decubitus PCD CTM (*B* and *D*) demonstrate opacification of a paraspinal vein (*B*, *arrow*) and the azygous and hemiazygous vein (*D*, *arrow*), consistent with a CVF. Axial 40-keV images at the same slices obtained 30 seconds later (*C* and *E*) no longer show contrast within these veins (*C* and *E*, *arrows*). The patient underwent transvenous Onyx embolization of the left T10 CVF.

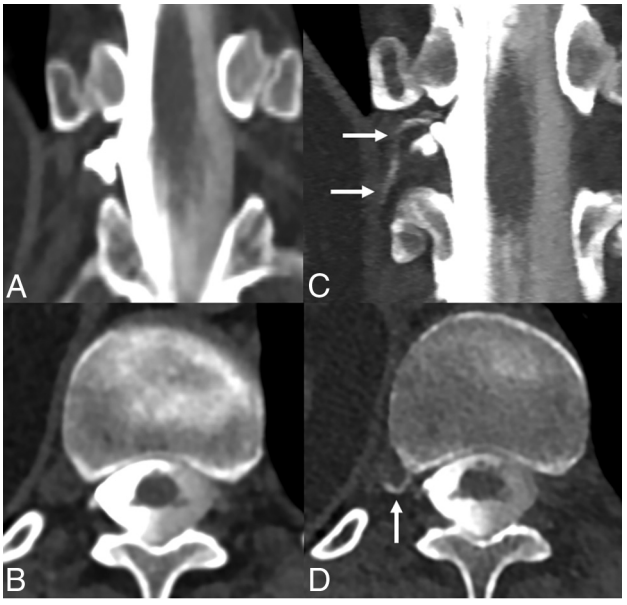

FIG 5. A 55-year-old woman with SIH according to the ICHD-3 criteria, including dural enhancement and venous distention on brain MR imaging (not shown). Coronal and axial images from a right lateral decubitus dynamic CTM (*A* and *B*) on an EID scanner reconstructed at 0.6 mm show no clear CVF. Subsequent PCD CTM with the patient in the right lateral decubitus position, including 0.2-mm coronal and axial reconstructions (*C* and *D*), shows a clear right T11 CVF (*C* and *D*, *arrows*).

and respiratory instructions during imaging.[3,4,10] Some institutions prefer a 2-day myelographic technique, while others perform a same-day bilateral technique.[11] Despite considerable improvement in technique at many centers, CVFs can be missed, even in patients meeting the ICHD-3 criteria for SIH with no evidence of type 1 or 2 leaks. Our series suggests that PCD CTM could have a role in identifying CVFs in patients with negative findings on DSM or dynamic EID CTM (Figs 2–6). Furthermore, PCD CTM may be a reasonable initial myelographic test to localize CVFs as this technology becomes more accessible (Fig 1).

PCD CTM may theoretically be more sensitive for CVF detection for many reasons. First, it has superior spatial resolution compared with the most current EID scanners. PCD CT allows an axial section thickness of 0.2–0.4 mm (depending on the scan mode) compared with 0.6 mm on most modern EID CT scanners. This permits more exquisite visualization of tiny veins draining a CVF, or in some cases, it simply allows better discrimination of a thin contrast column within a vein (Figs 1 and 6). Some previously reported CVFs drain predominantly into the internal epidural venous plexus, and high spatial resolution may be particularly beneficial to evaluate these.[12] Second, PCD CT allows simultaneous spectral and high-spatial-resolution imaging with decreased noise. While EID-based dual-energy CT scanners can also create VMIs, the spatial resolution and SNR are inferior. One study on EID CT suggested that 50-keV VMIs offer the best SNR.[13] In our series, monoenergetic reconstructions as low as 40 keV retained acceptable noise while maximizing iodine conspicuity (Figs 1–4). Finally, PCD CT has excellent temporal resolution, with an average scan length of 5.0 seconds in SR mode in this study, though scan lengths are longer in the UHR mode. This high temporal resolution minimizes motion degradation of images and permits sampling of multiple time points during a relatively short interval. While EID CT can achieve similar scan speeds, it cannot simultaneously provide high spatial resolution, and obtaining VMIs with a dual-energy technique usually requires slower scan modes.[8]

Certainly, further study will be needed to definitively determine whether PCD CTM provides superior sensitivity for CVF detection. Nonetheless, we believe the combination of high temporal and spatial resolution, as well as the spectral imaging capabilities allowed by photon energy thresholding, may make PCD CTM more sensitive. While many modalities provide these advantages in isolation, PCD CTM confers all of them in concert.

Our study has limitations, the most noteworthy being its small sample size. Because PCD CT is relatively new in our clinical practices, access to these scanners is limited, and we have been able to offer this examination to only a small number of patients. Further study will be needed once our patient database grows. Additionally, not all 6 patients underwent the exact same myelographic work-up, and there was some variation in precise examination techniques. Although we believe that the superior imaging provided by PCD CT aided in the detection of CVFs in patients 2–6, there are many other factors that influence the conspicuity

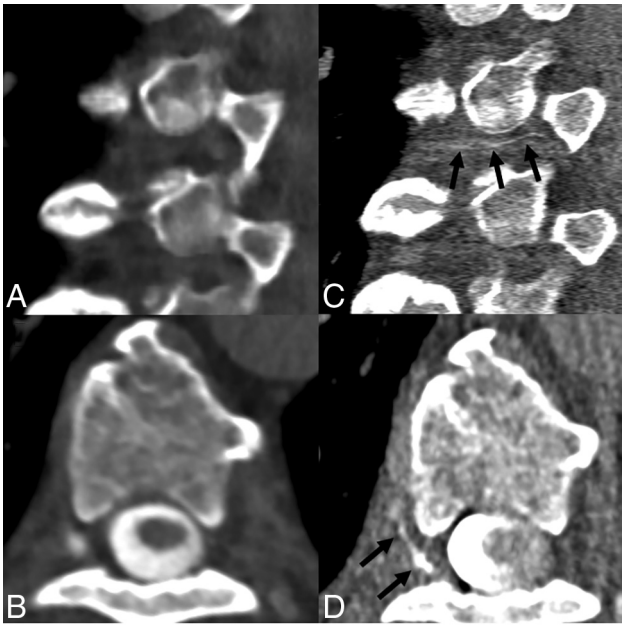

FIG 6. A 65-year-old woman with SIH confirmed by the ICHD-3 criteria, as well as brain MR imaging showing dural enhancement and venous distention (not shown). Sagittal and axial images during decubitus dynamic EID CTM (*A* and *B*, 0.625-mm section thickness) show no evidence of a CVF. Subsequent right lateral decubitus PCD CTM (*C* and *D*, 0.2-mm section thickness) demonstrates a clear right T6 CVF (*C* and *D*, *arrows*).

of CVFs, such as timing between contrast injection and imaging. CVF conspicuity can fluctuate on the order of seconds, and this fluctuation could confound our findings.[14] There was also variation in the number of scans obtained during each PCD CTM; further study on the temporal characteristics of CVFs will be helpful to determine how many are actually needed. This will help minimize the radiation dose as the examination technique is refined. For reference, the dose for PCD CTM in patients 1–4 was generally higher than the reported doses for dynamic EID CTM in the literature (which, in turn, is higher than reported doses for DSM), likely due to the high number of scans obtained.[15,16]

As PCD CTM becomes increasingly available, a more consistent imaging protocol can be developed. This will allow prospective and more precise comparison among LDDSM, EID CTM, and PCD CTM. Despite its limitations, our study suggests that PCD CTM has the potential to improve the diagnosis of CVFs, and additional investigation of this technique may prove useful to patients.

ACKNOWLEDGMENT

This work was a collaboration between the Mayo Clinic and Duke Health. The authors acknowledge the support of the Mayo Clinic CT Clinical Innovation Center and Siemens, who owns the PCD CT system used at the Mayo Clinic. No funding was used for the present study.

Disclosure forms provided by the authors are available with the full text and PDF of this article at www.ajnr.org.

REFERENCES

1. Schievink WI, Maya MM, Jean-Pierre S, et al. **A classification system of spontaneous spinal CSF leaks.** *Neurology* 2016;87:673–79 CrossRef Medline
2. Kranz PG, Gray L, Amrhein TJ. **Decubitus CT myelography for detecting subtle CSF leaks in spontaneous intracranial hypotension.** *AJNR Am J Neuroradiol* 2019;40:754–56 CrossRef Medline
3. Mamlouk MD, Ochi RP, Jun P, et al. **Decubitus CT myelography for CSF-venous fistulas: a procedural approach.** *AJNR Am J Neuroradiol* 2021;42:32–36 CrossRef Medline
4. Mark IT, Amans MR, Shah VN, et al. **Resisted inspiration: a new technique to aid in the detection of CSF-venous fistulas.** *AJNR Am J Neuroradiol* 2022;43:1544–47 CrossRef Medline
5. Amrhein TJ, Gray L, Malinzak MD, et al. **Respiratory phase affects the conspicuity of CSF-venous fistulas in spontaneous intracranial hypotension.** *AJNR Am J Neuroradiol* 2020;41:1754–56 CrossRef Medline
6. Madhavan AA, Cutsforth-Gregory JK, Benson JC, et al. **Conebeam CT as an adjunct to digital subtraction myelography for detection of CSF-venous fistulas.** *AJNR Am J Neuroradiol* 2023;44:347–50 CrossRef Medline
7. Leng S, Bruesewitz M, Tao S, et al. **Photon-counting detector CT: system design and clinical applications of an emerging technology.** *Radiographics* 2019;39:729–43 CrossRef Medline
8. Rajendran K, Petersilka M, Henning A, et al. **First clinical photon-counting detector CT system: technical evaluation.** *Radiology* 2022;303:130–38 CrossRef Medline
9. Schwartz FR, Malinzak MD, Amrhein TJ. **Photon-counting computed tomography scan of a cerebrospinal fluid venous fistula.** *JAMA Neurol* 2022;79:628–29 CrossRef Medline
10. Kim DK, Brinjikji W, Morris PP, et al. **Lateral decubitus digital subtraction myelography: tips, tricks, and pitfalls.** *AJNR Am J Neuroradiol* 2020;41:21–28 CrossRef Medline
11. Carlton Jones L, Goadsby PJ. **Same-day bilateral decubitus CT myelography for detecting CSF-venous fistulas in spontaneous intracranial hypotension.** *AJNR Am J Neuroradiol* 2022;43:645–48 CrossRef Medline
12. Kranz PG, Gray L, Malinzak MD, et al. **CSF-venous fistulas: anatomy and diagnostic imaging.** *AJR Am J Roentgenol* 2021;217:1418–29 CrossRef Medline
13. Albrecht MH, Vogl TJ, Martin SS, et al. **Review of clinical applications for virtual monoenergetic dual-energy CT.** *Radiology* 2019;293:260–71 CrossRef Medline
14. Mark I, Madhavan A, Oien M, et al. **Temporal characteristics of CSF-venous fistulas on digital subtraction myelography.** *AJNR Am J Neuroradiol* 2023;44:492–95 CrossRef Medline
15. Mamlouk MD, Shen PY, Dahlin BC. **Modified dynamic CT myelography for type 1 and 2 CSF leaks: a procedural approach.** *AJNR Am J Neuroradiol* 2023;44:341–46 CrossRef Medline
16. Nicholson PJ, Guest WC, van Prooijen M, et al. **Digital subtraction myelography is associated with less radiation dose than CT-based techniques.** *Clin Neuroradiol* 2021;31:627–31 CrossRef Medline